Journal of Engineering Mathematics, Vol. 10, No. 4, October 1976
Noordhoff International Publishing–Leyden
Printed in The Netherlands

Stokes flow for a stokeslet between two parallel flat plates

N. LIRON and S. MOCHON

Department of Applied Mathematics, The Weizmann Institute of Science, Rehovot, Israel

(Received June 2, 1975 and in revised form August 20, 1975)

SUMMARY

Velocity and pressure fields for Stokes flow due to a force singularity of arbitrary orientation and arbitrary distance between two parallel plates are found, using the image technique and a Fourier transform. Two alternative expressions for the solution, one in terms of infinite integrals and the other in terms of infinite series, are given. The infinite series solution is especially suitable for computation purposes being an exponentially decreasing series. From the series the "far field" behaviour is extracted. It is found that a force singularity parallel to the two planes has a far field behaviour of source and image for the parallel components (a two dimensional source doublet of height-dependent strength) whereas the normal component, and all fields due to a force singularity normal to the planes, die out exponentially. Velocity fields are compared with those of the one plane case. An estimate of the influence of the second wall and when its effect can be disregarded is obtained.

1. Introduction

In a wide range of animal and plant structures, the outer cells of a surface have hair-like extensions called cilia. These cilia move in an organized fashion to produce flow in the fluid which is bathing them.

Among the diverse physiological processes in which this ciliary motion plays an important role are the propulsion of micro-organisms, feeding and respiration in plants, and transport of mucous in the respiratory system and of gametes in the reproductive system.

To understand how ciliary motion performs its functions some theoretical work has been done. The first kind of approach that was taken is the so called "envelope model", which replaces the cilia by a waving wall. This model has been used by Blake [2] to model ciliated micro-organisms, by Lardner and Shack [5] in modeling fluid transport in tubules and by Ross [8] to model mucous flow in the lung. Results obtained using this model are sometimes very poor. For example according to this model velocities of propulsion in micro-organisms cannot exceed about half the wave speed, contrary to observation. This is because the envelope approach is appropriate only for Symplectic metachronism where the cilia are closely packed together. In Antiplectic metachronism, cilia are very spread out during the effective stroke and thus the envelope model is not suitable. The individuality of the cilium must be considered. A more recent approach developed by Blake [3], the "cilia sublayer model" takes this into account. Each cilium is represented by a line of force singularities in order to first obtain the velocity field due to a single cilium. An expression for the total velocity field is then found by summing the contributions of all the cilia. Blake [3] uses this approach in modeling propulsion of micro-organisms.

Due to the line of force singularities introduced in this kind of approach, the Green's function for the velocity field in the region of consideration has to be known. If the application is propulsion of micro-organisms the solution for a force singularity (stokeslet) in the vicinity of a flat plate is needed and has been given by Blake [1] and previously by Lorentz [6]. However, if the application in mind is for example in ciliated tubes, the stokeslet singularity has to be studied in a confined region. Using the envelope model, Lardner and Shack [5] calculated the flow of sperm through the ductus efferents of the male reproductive tract, obtaining results of about 50 times smaller than the observed ones. This is an indication that the envelope model is not appropriate so the second approach has to be used. For this purpose in this work the solution for a stokeslet between two parallel plates is given. De Mestre [7] adapted Faxen's technique to solve for a stokeslet parallel, and midway, between two flat plates. This he used to solve for a slender cylindrical cylinder falling parellel and midway between the two plates, either horizontally or vertically. The present work extends his solution to the case when the stokeslet is located at an arbitrary distance between the walls, and is of arbitrary orientation.

The problem is formulated in Section 2. In Section 3 the first part of the solution due to repeated reflections of the source in the two planes, is computed. The auxiliary solution to get no-slip conditions on the two plates is found in Section 4 using a Fourier transform, thus yielding the complete solution in terms of infinite integrals. The solution is transformed into an infinite series, in Section 5, integrating over the Hankel contour in the complex plane. The resulting series are exponentially decreasing and therefore most suitable for computational purposes. In Section 6, these series are used to compute the velocity fields for various distances between the plates. The resulting fields are then compared with those of the one plane case.

Since the problem and method of solution is similar to that of Blake [1], we shall use Blake's notation as far as possible in order to make the paper easier to follow.

2. Formulation of problem

Consider a force singularity (stokeslet) in a viscous incompressible fluid between two parallel flat plates a distance H apart, and choose a cartesian coordinate system (x_1, x_2, x_3) such that the plates are defined by $x_3 = 0$, and $x_3 = H\ (> 0)$, see Figure 1. We are looking for the fundamental singular solutions (velocity and pressure) of the stokeslet situated at $(y_1, y_2, y_3) = (y_1, y_2, h)$, satisfying the no-slip boundary conditions on the two planes. The three solutions for the pressure and the velocity, respectively

$$P^k,\ \boldsymbol{u}^k = (u_j^k), \qquad j = 1, 2, 3, \quad k = 1, 2, 3, \tag{1}$$

correspond to a stokeslet in the k-direction, and are the solutions of the Stokes equations

$$\nabla P^k = \mu \nabla^2 \boldsymbol{u}^k + \delta(\boldsymbol{x} - \boldsymbol{y})\boldsymbol{e}^k, \tag{2}$$

$$\nabla \cdot \boldsymbol{u}^k = 0, \tag{3}$$

with the boundary conditions

$$\boldsymbol{u}^k(x_1, x_2, 0) = \boldsymbol{u}^k(x_1, x_2, H) = 0. \tag{4}$$

Here $\boldsymbol{e}^k$ is a unit vector in the k-direction, and μ is viscosity.

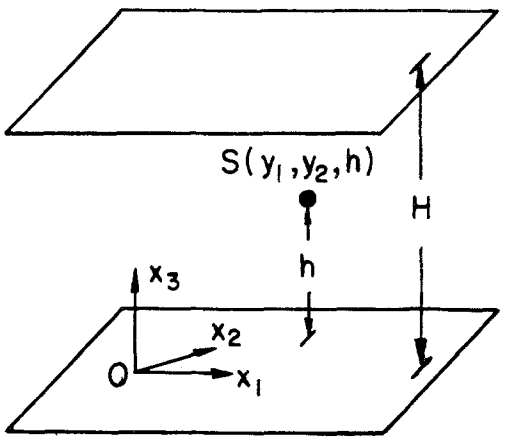

Figure 1. Configuration of the problem. The stokeslet situated at S.

The solution to equations (2), (3), in an infinite fluid (i.e., solution decaying to zero at infinity) is given by

$$\tilde{u}_j^k = \frac{1}{8\pi\mu}\left[\frac{\delta_{jk}}{|x-y|} + \frac{(x_j - y_j)(x_k - y_k)}{|x-y|^3}\right], \tag{5}$$

$$\tilde{p}^k = \frac{1}{4\pi}\frac{x_k - y_k}{|x-y|^3}, \tag{6}$$

where $|x - y|$ is the distance between x and y, see e.g., Blake [1]. This solution takes care of the singularity and we are left to solve for the correction, i.e., to solve for

$$\nabla\tilde{q}^k = \mu\nabla^2\tilde{v}^k, \tag{7}$$

$$\nabla\cdot\tilde{v} = 0, \tag{8}$$

with the boundary conditions

$$\tilde{v}_j^k = -\tilde{u}_j^k, \text{ on } x_3 = 0, H,$$

$\tilde{u}_j^k$ given by eq. (5).

3. Reflection images of the source

For the case of one plate (equivalent to $H \to \infty$) this problem has been solved by Blake [1] taking the image and an additional correction. The image is taken first to simplify the analysis as five of the nine components of u_j^k are then already zero on the boundary. For the case of two plates this "first" image corrects the boundary conditions on one plate—but disturbs the boundary conditions on the other plate. A multiple reflection has to be taken in order to get the same five components of u_j^k zero on both boundaries, see Fig. 2. It is tempting to go one step further and multiply reflect the entire Blake solution in order to achieve the no-slip conditions on both plates. Unfortunately the additional correction has the distance from one of the plates, h, explicitly appearing in it and simple repeated reflec-

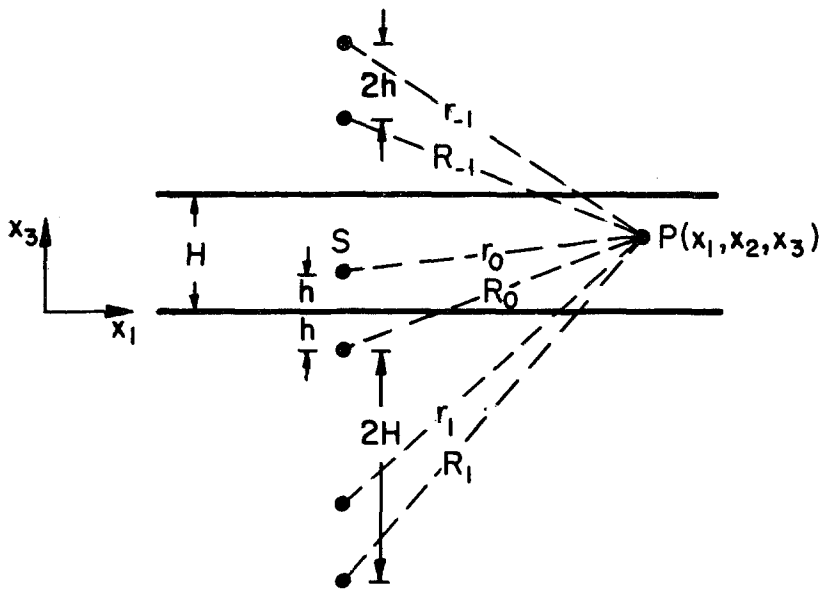

Figure 2. Source and first few images (in pairs), a side view.

tions does not work. We shall therefore first take the repeated reflection solution of equation (5), and then solve for the correction using a two dimensional Fourier transform similar to that used by Blake [1]. The velocity induced by the source together with all image reflections is given by

$$v_j^k = \frac{1}{8\pi\mu} \sum_{n=-\infty}^{\infty} \left[\left(\frac{1}{r_n} - \frac{1}{R_n} \right) \delta_{jk} + \frac{r_{nj} r_{nk}}{r_n^3} - \frac{R_{nj} R_{nk}}{R_n^3} \right], \tag{10}$$

and the pressure by

$$q^k = \frac{1}{4\pi} \sum_{n=-\infty}^{\infty} \left(\frac{r_{nk}}{r_n^3} - \frac{R_{nk}}{R_n^3} \right), \tag{10a}$$

where $r_n = |\boldsymbol{r}_n|$, $R_n = |\boldsymbol{R}_n|$. The vectors $\boldsymbol{r}_n$, $\boldsymbol{R}_n$ defined by

$$\begin{aligned} \boldsymbol{r}_n &= (r_{n1}, r_{n2}, r_{n3}) = (x_1 - y_1, x_2 - y_2, x_3 - h + 2nH), \\ \boldsymbol{R}_n &= (R_{n1}, R_{n2}, R_{n3}) = (x_1 - y_1, x_2 - y_2, x_3 + h + 2nH), \qquad n = 0, \pm 1, \pm 2, \ldots \end{aligned} \tag{11}$$

are vectors from the source images to the point $\boldsymbol{x}$.

Note that v_j^k and q^k are solutions of equations (2) and (3), since all images ($n \neq 0$ terms and R_0) have their sources outside the region $0 \leqq x_3 \leqq H$, and therefore satisfy equations (7), (8) in the above region.

Using the Lipshitz integral (see Watson [10], page 384)

$$\frac{1}{(\rho^2 + a^2)^{\frac{1}{2}}} = \int_0^{\infty} J_0(\rho\lambda) e^{-|a|\lambda} d\lambda, \tag{12}$$

one derives the following results:

$$\sum_{n=-\infty}^{\infty}\left(\frac{1}{r_n}-\frac{1}{R_n}\right)=2\int_0^\infty J_0(\lambda\rho)\frac{\sinh\lambda h}{\sinh\lambda H}\sinh\lambda(H-x_3)\,d\lambda,$$
$$\rho^2=(x_1-y_1)^2+(x_2-y_2)^2,\qquad x_3>h, \tag{13}$$

and for $x_3 < h$ replace h by $H - h$ and x_3 by $H - x_3$, i.e.,

$$\sum_{n=-\infty}^{\infty}\left(\frac{1}{r_n}-\frac{1}{R_n}\right)=2\int_0^\infty J_0(\lambda\rho)\frac{\sinh\lambda(H-h)}{\sinh\lambda H}\sinh\lambda x_3\,d\lambda,\qquad x_3<h. \tag{14}$$

Using equations (13) and (14) one gets for v_j^k the expression,

$$\begin{aligned}4\pi\mu v_j^k &= \delta_{jk}\int_0^\infty J_0(\lambda\rho)\frac{\sinh\lambda h}{\sinh\lambda H}\sinh\lambda(H-x_3)\,d\lambda\\
&+\delta_{j\alpha}\delta_{k\beta}\frac{r_\alpha r_\beta}{\rho}\int_0^\infty \lambda J_1(\lambda\rho)\frac{\sinh\lambda h}{\sinh\lambda H}\sinh\lambda(H-x_3)\,d\lambda\\
&-\delta_{j3}\delta_{k3}\int_0^\infty \lambda J_0(\lambda\rho)\frac{d}{d\lambda}\left[\frac{\sinh\lambda h}{\sinh\lambda H}\sinh\lambda(H-x_3)\right]d\lambda\\
&+\operatorname{sgn}(x_3-h)(\delta_{j3}\delta_{k\alpha}+\delta_{j\alpha}\delta_{k3})r_\alpha\int_0^\infty \lambda J_0(\lambda\rho)\frac{\sinh\lambda h}{\sinh\lambda H}\cosh\lambda(H-x_3)\,d\lambda,\\
&\qquad\qquad x_3>h.\end{aligned} \tag{15}$$

Here and henceforth α, β take on the values 1 or 2 only. For $x_3 < h$ replace x_3 by $H - x_3$ and h by $H - h$ under the integral signs only.

The corresponding pressure is

$$\begin{aligned}2\pi q^k &= \frac{r_\alpha}{\rho}\delta_{k\alpha}\int_0^\infty \lambda J_1(\lambda\rho)\frac{\sinh\lambda h}{\sinh\lambda H}\sinh\lambda(H-x_3)\,d\lambda\\
&+\operatorname{sgn}(x_3-h)\delta_{k3}\int_0^\infty \lambda J_0(\lambda\rho)\frac{\sinh\lambda h}{\sinh\lambda H}\cosh\lambda(H-x_3)\,d\lambda,\qquad x_3>h.\end{aligned} \tag{16}$$

For $x_3 < h$ replace x_3 by $H - x_3$, h by $H - h$ under the integral signs only.

The velocities v_j^k satisfy the following conditions on the two plates:

$$\begin{aligned}4\pi\mu v_j^k(x_3=0) &= -(\delta_{j3}\delta_{k\alpha}+\delta_{j\alpha}\delta_{k3})r_\alpha\int_0^\infty \lambda J_0(\lambda\rho)\frac{\sinh\lambda(H-h)}{\sinh\lambda H}\,d\lambda,\\
4\pi\mu v_j^k(x_3=H) &= (\delta_{j3}\delta_{k\alpha}+\delta_{j\alpha}\delta_{k3})r_\alpha\int_0^\infty \lambda J_0(\lambda\rho)\frac{\sinh\lambda h}{\sinh\lambda H}\,d\lambda.\end{aligned} \tag{17}$$

Again it is emphasized that α takes on the values 1, 2 only. We therefore have to solve for the correction, again equation (7) and (8), but now with the negative of the boundary conditions (17). This will be done in the next section.

4. Auxiliary solution

To solve equations (7) and (8) with the negative of the boundary values (17), we shall use the two dimensional Fourier transform

$$\hat{\phi}(\lambda_1, \lambda_2, x_3) = \frac{1}{2\pi} \int_{-\infty}^{\infty} \int_{-\infty}^{\infty} \phi(r_1, r_2, x_3) e^{i(\lambda_1 r_1 + \lambda_2 r_2)} dr_1 dr_2. \tag{18}$$

The transformed equations of momentum conservation (7) become

$$-i\lambda_\alpha \delta_{\alpha j} \hat{S}^k + \delta_{j3} \frac{\partial \hat{S}^k}{\partial x_3} = \mu L(\hat{w}_j^k), \tag{19}$$

the transformed continuity equation (8),

$$-i\lambda_\alpha \hat{w}_\alpha^k + \frac{\partial \hat{w}_3^k}{\partial x_3} = 0, \tag{20}$$

and since a necessary condition is that the pressure must satisfy $\nabla^2 S^k = 0$, this transforms into

$$L(\hat{S}^k) = 0. \tag{21}$$

Here

$$L = \frac{\partial^2}{\partial x_3^2} - \xi^2, \qquad \xi^2 = \lambda_1^2 + \lambda_2^2, \tag{22}$$

and the Einstein summation convention is used; see also Blake [1].

Transforming the boundary conditions (17), we note that

$$\hat{v}_j^k(x_3 = 0, H) = -i \frac{\partial}{\partial \lambda_l} \widehat{(v_j^k / r_l)}, \qquad l = 1, 2. \tag{23}$$

Both conditions in (17) are of the form

$$\int_0^\infty \lambda J_0(\lambda \rho) f(\lambda) d\lambda, \tag{24}$$

which can be looked upon as the (inverse) zero order Hankel transform. By Sneddon [9] the double Fourier transform equals the zero order Hankel transform if $\phi(r_1, r_2, x_3) = \phi_1[(r_1^2 + r_2^2)^{\frac{1}{2}}, x_3] = \phi_1(\rho, x_3)$. We thus get for the transformed boundary conditions of w_j^k:

$$\begin{aligned} 4\pi\mu \hat{w}_j^k(x_3 = 0) &= -i(\delta_{j3}\delta_{k\alpha} + \delta_{j\alpha}\delta_{k3}) \frac{\partial}{\partial \lambda_\alpha} \left[\frac{\sinh \xi(H - h)}{\sinh \xi H} \right], \\ 4\pi\mu \hat{w}_j^k(x_3 = H) &= i(\delta_{j3}\delta_{k\alpha} + \delta_{j\alpha}\delta_{k3}) \frac{\partial}{\partial \lambda_\alpha} \left[\frac{\sinh \xi h}{\sinh \xi H} \right]. \end{aligned} \tag{25}$$

The general solution to eq. (21) can be written as

$$\hat{S}^k = B^k \sinh \xi(H - x_3) + C^k \cosh \xi(H - x_3), \tag{26}$$

and the solution to eq. (19) is then

$$2\mu\hat{w}_j^k = B_j^k \sinh \xi(H - x_3) + C_j^k \cosh \xi(H - x_3)$$
$$+ (B^k\delta_{j3} + C^k\delta_{\alpha j} i\lambda_\alpha/\xi)x_3 \sinh \xi(H - x_3)$$
$$+ (C^k\delta_{j3} + B^k\delta_{\alpha j} i\lambda_\alpha/\xi)(x_3 - H) \cosh \xi(H - x_3). \tag{27}$$

The coefficients B^k, C^k are found in terms of B_j^k, C_j^k. By inserting eq. (27) into the transformed continuity equation (20), we get the coupled equations

$$\begin{aligned} C^k &= \xi H B^k + \xi B_3^k + i\lambda_\beta C_\beta^k, \\ B^k &= -\xi H C^k + \xi C_3^k + i\lambda_\beta B_\beta^k. \end{aligned} \tag{28}$$

We then insert these expressions into the conditions (25) and finally get

$$2\pi B^k = [\sinh^2 \xi H - (\xi H)^2]^{-1}$$
$$\cdot\Big\{ i\lambda_\alpha\delta_{\alpha k}\Big[\sinh^2 \xi H \frac{d}{d\xi}\Big(\frac{\sinh \xi h}{\sinh \xi H}\Big) + \xi H \sinh \xi H \frac{d}{d\xi}\Big(\frac{\sinh \xi(H - h)}{\sinh \xi H}\Big)\Big]$$
$$+ \delta_{k3}\xi[\xi hH \sinh \xi(H - h) - (H - h) \sinh \xi h \sinh \xi H]\Big\}, \tag{29}$$

and

$$2\pi C^k = [\sinh^2 \xi H - (\xi H)^2]^{-1}$$
$$\cdot\Big\{ i\lambda_\alpha\delta_{\alpha k}[\xi hH \sinh \xi(H - h) + (H - h) \sinh \xi h \sinh \xi H]$$
$$- \delta_{k3}\xi\Big[\sinh^2 \xi H \frac{d}{d\xi}\Big(\frac{\sinh \xi h}{\sinh \xi H}\Big) - \xi H \sinh \xi H \frac{d}{d\xi}\Big(\frac{\sinh \xi(H - h)}{\sinh \xi H}\Big)\Big]\Big\}. \tag{30}$$

The transformed velocity is then,

$$\hat{w}_j^k = \frac{i}{4\pi\mu}(\delta_{j3}\delta_{k\alpha} + \delta_{j\alpha}\delta_{k3})(\lambda_\alpha/\xi)$$
$$\cdot\Big\{(H - h)\frac{\sinh \xi h \sinh \xi(H - x_3)}{\sinh \xi H} + \frac{d}{d\xi}\Big(\frac{\sinh \xi h}{\sinh \xi H}\Big)\cosh \xi(H - x_3)\Big\}$$
$$+ \frac{1}{2\mu}[B^k\delta_{j3} + C^k i\delta_{\alpha j}\lambda_\alpha/\xi]x_3 \sinh \xi(H - x_3)$$
$$+ \frac{1}{2\mu}[C^k\delta_{\alpha 3} + B^k i\delta_{\alpha j}\lambda_\alpha/\xi][x_3 \cosh \xi(H - x_3) - H \sinh \xi x_3/\sinh \xi H]. \tag{31}$$

To get S^k and w_j^k one has to take the two dimensional inverse Fourier transform which is again the Hankel transform of order zero. It is easier to separate the cases for j and k not equal to three, one of them equal to three and both three. For j and k not equal to three we have (since $\hat{w}_\alpha^\beta$ has an $i\lambda_\alpha i\lambda_\beta$ component)

$$w_\alpha^\beta = -\int_0^\infty \frac{\partial^2}{\partial r_\beta \partial r_\alpha}[(\lambda_\alpha\lambda_\beta)^{-1}\hat{w}_\alpha^\beta(\xi)\xi J_0(\rho\xi)]d\xi$$

$$= -\frac{1}{4\pi\mu}\frac{\partial}{\partial r_\beta}\frac{r_\alpha}{\rho}\int_0^\infty \xi J_1(\rho\xi)A_1(\xi)d\xi, \tag{32}$$

where

$$A_1(\xi) = [\sinh^2 \xi H - (\xi H)^2]^{-1}\Big\{\xi h H x_3 \sinh \xi(H - x_3)\sinh \xi(H - h)$$

$$+ x_3[h \sinh \xi H \cosh \xi(H - x_3 - h) - H \sinh \xi h \cosh \xi x_3]$$

$$+ \xi H x_3 \sinh \xi H \cosh \xi(H - x_3)\frac{d}{d\xi}\left(\frac{\sinh \xi(H - h)}{\sinh \xi H}\right)$$

$$- H \sinh \xi x_3\left[\sinh \xi H \frac{d}{d\xi}\left(\frac{\sinh \xi h}{\sinh \xi H}\right) + \xi H \frac{d}{d\xi}\left(\frac{\sinh \xi(H - h)}{\sinh \xi H}\right)\right]\Big\}. \tag{33}$$

$A_1(\xi)$ in equation (33) has already been brought into a form insuring convergence of the integral in equation (32). For $j = k = 3$,

$$w_3^3 = \int_0^\infty \xi J_0(\rho\xi)\hat{w}_3^3(\xi)d\xi = \frac{1}{4\pi\mu}\int_0^\infty J_0(\rho\xi)A_2(\xi)d\xi, \tag{34}$$

where

$$A_2(\xi) = \xi^2[\sinh^2 \xi H - (\xi H)^2]^{-1}\Big\{x_3\Big[H \sinh \xi h \cosh \xi x_3$$

$$- h \sinh \xi H \cosh \xi(H - x_3 - h) + \xi h H \sinh \xi(H - x_3)\sinh \xi(H - h)$$

$$+ \xi H \cosh \xi(H - x_3)\sinh \xi H \frac{d}{d\xi}\left(\frac{\sinh \xi(H - h)}{\sinh \xi H}\right)\Big]$$

$$- \xi H^2 \sinh \xi x_3 \frac{d}{d\xi}\left(\frac{\sinh \xi(H - h)}{\sinh \xi H}\right)$$

$$+ H \sinh \xi x_3 \sinh \xi H \frac{d}{d\xi}\left(\frac{\sinh \xi h}{\sinh \xi H}\right)\Big\}, \tag{35}$$

with the same comment concerning $A_2(\xi)$.

For $j = 3$ (first pair of indices) or $k = 3$ (second pair) we get

$$w_{3,\alpha}^{\alpha,3} = -\frac{\partial}{\partial r_\alpha}\int_0^\infty \xi J_0(\rho\xi)(i\lambda_\alpha)^{-1}\hat{w}_{3,\alpha}^{\alpha,3}(\xi)d\xi$$

$$= -\frac{1}{4\pi\mu}\frac{\partial}{\partial r_\alpha}\int_0^\infty J_0(\rho\xi)[A_3(\xi) + A_4(\xi)]d\xi, \tag{36}$$

where

$$
\begin{aligned}
A_3(\xi) &= (\sinh^2 \xi H)^{-1}[h \sinh \xi H \cosh \xi(H - x_3 - h) - H \sinh \xi h \cosh \xi x_3], \\
A_4(\xi) &= \xi[\sinh^2 \xi H - (\xi H)^2]^{-1}\{x_3 \xi H[h \sinh \xi(x_3 - h) \\
&\quad + H \sinh \xi h \sinh \xi(H - x_3)/\sinh \xi H] \\
&\quad - \xi h H^2 \sinh \xi x_3 \sinh \xi(H - h)/\sinh \xi H \\
&\quad + (\delta_{j3} - \delta_{k3})[-H(H - h) \sinh \xi h \sinh \xi x_3 + x_3(h \sinh \xi H \sinh \xi(H - x_3 - h) \\
&\quad + H \sinh \xi h \sinh \xi x_3)]\}.
\end{aligned} \tag{37}
$$

The contribution of $A_3(\xi)$ in (36), combines with the last term in equation (15), i.e., the term giving rise to the non-zero boundary values (17), to yield the desired boundary condition (4). We obtain for their sum

$$
\frac{1}{4\pi\mu}(x_3 - h)(r_\alpha/\rho)(\delta_{j3}\delta_{k\alpha} + \delta_{j\alpha}\delta_{k3}) \int_0^\infty \xi J_1(\rho\xi) \frac{\sinh \xi h \sinh \xi(H - x_3)}{\sinh \xi H} \, d\xi, \qquad x_3 > h, \tag{38}
$$

and h replaced by $H - h$, x_3 replaced by $H - x_3$ under the integral sign, for $x_3 < h$.

For the pressure we get

$$
S^k = \frac{1}{2\pi} \int_0^\infty \left[\frac{r_\alpha}{\rho} J_1(\rho\xi) A_5(\xi) \delta_{k\alpha} + J_0(\rho\xi) A_6(\xi) \delta_{k3} \right] d\xi, \tag{39}
$$

where

$$
\begin{aligned}
A_5(\xi) &= \xi^2[\sinh^2 \xi H - (\xi H)^2]^{-1} \\
&\quad \cdot \Bigg\{ \left[\sinh \xi H \frac{d}{d\xi}\left(\frac{\sinh \xi h}{\sinh \xi H} \right) + \xi H \frac{d}{d\xi}\left(\frac{\sinh \xi(H - h)}{\sinh \xi H} \right) \right] \\
&\quad \cdot \sinh \xi H \sinh \xi(H - x_3) \\
&\quad + [\xi h H \sinh \xi(H - h) + (H - h) \sinh \xi h \sinh \xi H] \cosh \xi(H - x_3) \Bigg\}, \\
A_6(\xi) &= \xi^2[\sinh^2 \xi H - (\xi H)^2]^{-1} \\
&\quad \cdot \Bigg\{ [\xi h H \sinh \xi(H - h) - (H - h) \sinh \xi h \sinh \xi H] \sinh \xi(H - x_3) \\
&\quad - \left[\sinh \xi H \frac{d}{d\xi}\left(\frac{\sinh \xi h}{\sinh \xi H} \right) - \xi H \frac{d}{d\xi}\left(\frac{\sinh \xi(H - h)}{\sinh \xi H} \right) \right] \\
&\quad \cdot \sinh \xi H \cosh \xi(H - x_3) \Bigg\}.
\end{aligned} \tag{40}
$$

This completes the solution, i.e. $u_j^k = v_j^k + w_j^k$ and $p^k = q^k + S^k$.

It would be nice if one could take this solution, or the equivalent form in the next section, and deduce from them the types of image singularities that occur. Unfortunately it is far from being clear (at least to us) that one can give such a "physical" description at all. Just the first part of the solution already has an infinite number of stokeslet images. Therefore we shall not attempt here such a description. For the far field, i.e., $\rho/H \gg 1$ this is possible and will be done in the next section.

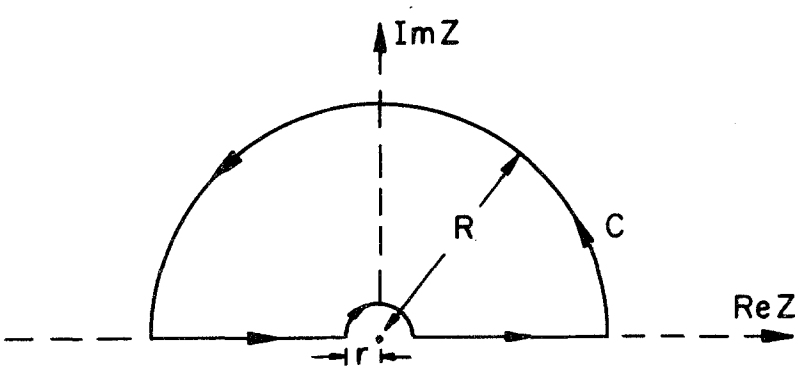

Figure 3. The Hankel contour, C, in the complex z plane.

5. Alternative form and the far field behaviour

Although the solution given in the previous section is complete it is difficult to evaluate the behaviour of the far field from it. In order to get a clear picture we shall transform the solution using the Hankel contour (Watson [10], p. 423), see Fig. 3. If we take the integral over the contour C in Fig. 3 as $r \to 0$, $R \to \infty$ of

$$\oint_C F(z) z^{\nu+1} H_\nu^{(1)}(bz)\, dz, \tag{41}$$

where b is real, $F(z)$ is an even function of z and $F(z)$ decays exponentially to zero on the real axis, as $x = \mathrm{Re}\, z \to \pm\infty$ we get

$$\int_0^\infty J_\nu(bx) x^{\nu+1} F(x)\, dx = \pi i \cdot (\text{sum of residues in upper half plane of } F(z) z^{\nu+1} H_\nu^{(1)}(bz)$$
$$\textit{including one half} \text{ of the residue at } z = 0). \tag{42}$$

These are not the most general conditions under which equation (42) holds, but it is sufficient for our case.

For the terms appearing in equations (15) and (38), the singularities of the functions are at $z_n = n\pi i/H$, $n = 1, 2, \ldots$ and $z = 0$ is not a singular point. All integrals can be expressed in terms of two integrals, and for them we obtain

$$\int_0^\infty J_0(x\rho) \frac{\sinh xh}{\sinh xH} \sinh x(H - x_3)\, dx = \frac{2}{H} \sum_{n=1}^{\infty} \sin\frac{n\pi h}{H} \sin\frac{n\pi x_3}{H} K_0\left(\frac{n\pi\rho}{H}\right), \tag{43}$$

and

$$\int_0^\infty xJ_1(x\rho)\frac{\sinh xh}{\sinh xH}\sinh x(H-x_3)dx$$

$$=\frac{2}{H}\sum_{n=1}^{\infty}\frac{n\pi}{H}\sin\frac{n\pi h}{H}\sin\frac{n\pi x_3}{H}K_1\left(\frac{n\pi\rho}{H}\right). \tag{44}$$

Notice that the restriction $x_3 > h$ can now be dropped. For the integrals involving $A_1(\xi)$, $A_2(\xi)$, $A_4(\xi)$, $A_5(\xi)$ and $A_6(\xi)$, three types of singularities appear. The first is a simple pole at $\xi = n\pi i/H$ coming from $1/\sinh \xi H$, the second is a double pole at $\xi = n\pi i/H$ coming from $1/\sinh^2 \xi H$, and the third type are simple poles coming from the roots of the equation

$$\sinh^2 z = z^2, \tag{45}$$

in the upper half plane (the behaviour at $\xi = 0$ needs a separate treatment).

The roots of equation (45) in the upper half plane are z_m and $-\bar{z}_m$ (bar denoting complex conjugate) where $z_m = x_m + iy_m$, $x_m > 0$, $y_m > 0$ and an asymptotic estimate for them is

$$z_m \sim \ln(2m+1)\pi + i(m+\tfrac{1}{2})\pi, \qquad m = 1, 2, \ldots. \tag{46}$$

The first six non-zero roots of equation (45) are given in Table 1.

TABLE 1

First six roots of the equation $\sinh^2 z = z^2$ *computed in the first quadrant*

n	$z_n = x_n + iy_n$
1	2.2507 + *i* 4.2124
2	2.7687 + *i* 7.4977
3	3.1031 + *i*10.7125
4	3.3522 + *i*13.8999
5	3.5511 + *i*17.0734
6	3.7168 + *i*20.2385

Applying transformation (42) to u_j^k we find; again separating the three above mentioned cases:

$$u_j^k = u_3^3 = -\frac{1}{4\pi\mu}\frac{\pi}{H}\operatorname{Im}\left\{\sum_{m=1}^{\infty}\frac{z_m H_0^{(1)}(\rho z_m/H)}{(1+z_m^2)^{\frac{1}{2}}-1}\right.$$

$$\cdot\left[[(1+z_m^2)^{\frac{1}{2}}+1]\left(\frac{x_3}{H}\sinh\frac{hz_m}{H}\cosh\frac{x_3 z_m}{H}+\frac{h}{H}\sinh\frac{x_3 z_m}{H}\cosh\frac{hz_m}{H}\right.\right.$$

$$\left.\left.-\frac{1}{z_m}\sinh\frac{x_3 z_m}{H}\sinh\frac{z_m h}{H}\right)-\frac{h}{H}\frac{x_3}{H}z_m\right.\cdot$$

$$\cdot\left((1+z_m^2)^{\frac{1}{2}}\cosh\frac{x_3+h}{H}z_m+\cosh\frac{x_3-h}{H}z_m-z_m\sinh\frac{x_3+h}{H}z_m\right)$$

$$-z_m\frac{x_3+h}{H}\sinh\frac{hz_m}{H}\sinh\frac{x_3z_m}{H}\Bigg]\Bigg\}, \tag{47}$$

where Im( ) stands for the imaginary part, and we take the square root in the first quadrant.

$$u_j^k=u_{3,\alpha}^{\alpha,3}=-\frac{1}{4\pi\mu}\frac{r_\alpha}{\rho}\frac{\pi}{H}\operatorname{Im}\left\{\sum_{m=1}^{\infty}\frac{z_mH_1^{(1)}(\rho z_m/H)}{(1+z_m^2)^{\frac{1}{2}}-1}\left[\frac{h}{H}\frac{x_3}{H}z_m\right.\right.$$

$$\cdot\left(\sinh\frac{x_3-h}{H}z_m\pm z_m\cosh\frac{x_3+h}{H}z_m\mp(1+z_m^2)^{\frac{1}{2}}\sinh\frac{x_3+h}{H}z_m\right)$$

$$+z_m\left(\frac{x_3}{H}\cosh\frac{x_3z_m}{H}\sinh\frac{hz_m}{H}-\frac{h}{H}\sinh\frac{x_3z_m}{H}\cosh\frac{hz_m}{H}\right)$$

$$\left.\left.+\sinh\frac{hz_m}{H}\sinh\frac{x_3z_m}{H}\left(\frac{h-x_3}{H}(1+z_m^2)^{\frac{1}{2}}\pm\left(\frac{x_3+h}{H}-1\right)\right)\right]\right\}, \tag{48}$$

where the top signs are taken for $j=3$, and the lower signs for $k=3$. Notice that only the contributions from the singularities of the third type remain. The contributions from the imaginary axis cancel with the contributions from equations (15) and (38), and there is no contribution from the origin. This is not the case for u_α^β. In this case we get

$$u_j^k=u_\alpha^\beta=\frac{1}{4\pi\mu}\frac{\partial}{\partial r_\beta}\frac{r_\alpha}{\rho}\frac{\pi}{H}\operatorname{Im}\left\{H\sum_{m=1}^{\infty}H_1^{(1)}\left(\frac{\rho z_m}{H}\right)\left[\frac{1}{z_m}\sinh\frac{hz_m}{H}\sinh\frac{x_3z_m}{H}\right.\right.$$

$$+\frac{x_3}{H}\cosh\frac{x_3z_m}{H}\sinh\frac{hz_m}{H}+\frac{h}{H}\cosh\frac{hz_m}{H}\sinh\frac{x_3z_m}{H}$$

$$-\frac{1}{(1+z_m^2)^{\frac{1}{2}}-1}\left[z_m\frac{x_3+h}{H}\sinh\frac{hz_m}{H}\sinh\frac{x_3z_m}{H}+\frac{x_3}{H}\frac{h}{H}z_m\right.$$

$$\left.\left.\left.\cdot\left(\cosh\frac{h-x_3}{H}z_m+z_m\sinh\frac{x_3+h}{H}z_m-(1+z_m^2)^{\frac{1}{2}}\cosh\frac{x_3+h}{H}z_m\right)\right]\right]\right\}$$

$$+\frac{1}{4\pi\mu}\frac{\partial}{\partial r_\beta}\frac{r_\alpha}{\rho}\sum_{n=1}^{\infty}\frac{4}{n\pi}\sin\frac{n\pi h}{H}\sin\frac{n\pi x_3}{H}K_1\left(\frac{n\pi\rho}{H}\right)$$

$$+\frac{1}{4\pi\mu}\delta_{\alpha\beta}\frac{4}{H}\sum_{n=1}^{\infty}\sin\frac{n\pi h}{H}\sin\frac{n\pi x_3}{H}K_0\left(\frac{n\pi\rho}{H}\right)$$

$$-\frac{H}{4\pi\mu}\frac{6x_3}{H}\frac{h}{H}\left(1-\frac{x_3}{H}\right)\left(1-\frac{h}{H}\right)\frac{\partial}{\partial r_\beta}\left(\frac{r_\alpha}{\rho^2}\right). \tag{49}$$

The first part of u_α^β comes from the singularities not on the imaginary axis, the other two from singularities on the imaginary axis, and the last term from the origin. Since we have the asymptotic expansions

$$H_\nu^{(1)}(z) \sim (2/\pi z)^{\frac{1}{2}} e^{i(z-\frac{1}{2}\nu\pi-\frac{1}{4}\pi)} \sum_{m=0}^{\infty} \frac{(-1)^m(\nu, m)}{(2iz)^{2m}},$$

$$K_\nu(z) \sim (\pi/2z)^{\frac{1}{2}} e^{-z} \sum_{m=0}^{\infty} \frac{(\nu, m)}{(2z)^{2m}}, \tag{50}$$

see Watson [10], p. 198, 202 respectively, we see that u_j^k decays exponentially with ρ if either j or k (or both) are equal to three. For $u_j^k = u_\alpha^\beta$ the only term that does not decay exponentially is the last term. Summarizing we obtain

$$\begin{aligned} u_j^k \sim & -\frac{3H}{\pi\mu}\frac{x_3}{H}\left(1-\frac{x_3}{H}\right)\frac{h}{H}\left(1-\frac{h}{H}\right)\frac{1}{\rho^2}\left[\tfrac{1}{2}\delta_{\alpha\beta}-\frac{r_\alpha r_\beta}{\rho^2}\right]\delta_{j\alpha}\delta_{k\beta} \\ & + \delta_{j3}\delta_{k3}\,O(\rho^{-\frac{1}{2}}e^{-\rho y_1/H}) + (\delta_{j3}\delta_{k\alpha}+\delta_{k3}\delta_{j\alpha})\,O\left(\frac{r_\alpha}{\rho}\rho^{-\frac{1}{2}}e^{-\rho y_1/H}\right) \\ & + \delta_{j\alpha}\delta_{k\beta}\left[O\left(\frac{r_\alpha}{\rho}\frac{r_\beta}{\rho}\rho^{-\frac{1}{2}}e^{-\rho y_1/H}\right)+O\left(\frac{r_\alpha}{\rho}\frac{r_\beta}{\rho}\rho^{-\frac{1}{2}}e^{-\rho\pi/H}\right)\right]. \end{aligned} \tag{51}$$

Here y_1 is the imaginary part of the first root of equation (45), given in Table 1.

Equation (51) shows the drastic effect of the walls on the source field behaviour. A stokeslet in the x_3 direction induces an exponentially decaying velocity field with $\rho/H = (x_1^2 + x_2^2)^{\frac{1}{2}}/H$. This holds also for the x_3 component of the velocity field induced by a stokeslet in the x_1 or x_2 directions (a stokeslet parallel to the plates). The parallel components of the velocity field induced by a parallel stokeslet decay like the sum of the source and an image, i.e., $O[(\rho/H)^{-2}]$.

A source in three dimensions with mass outflow M per unit time induces a flow field

$$u_i = \frac{M}{4\pi}\frac{r_i}{r^3}, \tag{52}$$

and a source doublet of vector strength and direction $\boldsymbol{D}$, induces a flow field

$$u_i = \frac{D_j}{4\pi}\left(-\frac{\delta_{ij}}{r^3}+\frac{3r_ir_j}{r^5}\right), \tag{53}$$

which one gets by taking the negative of the gradient of (52) in the chosen direction, see Blake and Chwang [4]. If we take a source in two dimensions, then the two dimensional flow field induced is

$$u_i = \frac{M}{2\pi}\frac{r_i}{r^2}, \tag{54}$$

and a two dimensional source doublet of vector strength and direction $\boldsymbol{D} = (D_1, D_2)$ would be

$$u_i = \frac{D_j}{2\pi}\left(-\frac{\delta_{ij}}{r^2}+\frac{2r_ir_j}{r^4}\right). \tag{55}$$

If we look at the leading term in (51) we see that for a parallel stokeslet the far field behaves like a two dimensional source doublet, in plates parallel to the two walls, with strength depending in a parabolic way on the distance between the two plates, and direction in the direction of the original stokeslet. The strength of the source doublet is

$$\frac{3}{\mu H}\,\frac{h}{H}\left(1-\frac{h}{H}\right)\frac{x_3}{H}\left(1-\frac{x_3}{H}\right),$$

where we are measuring distances in units of H, i.e., write $r_1 = H(r_1/H)$ etc.

To complete the alternative form of the solution we have to give the pressure in the transformed form. This is

$$\begin{aligned}
p^k = \Bigg\{ & \frac{3}{\pi H^2}\,\frac{r_\alpha/H}{(\rho/H)^2}\,\frac{h}{H}\left(1-\frac{h}{H}\right) - \frac{1}{2H^2}\,\frac{r_\alpha}{\rho}\,\mathrm{Im}\sum_{m=1}^{\infty} H_1^{(1)}\left(\frac{\rho z_m}{H}\right)\Bigg[\frac{z_m^2}{(1+z_m^2)^{\frac{1}{2}}-1}\cdot \\
& \cdot\left(\sinh\frac{hz_m}{H}\cosh\frac{x_3 z_m}{H} + \frac{h}{H}\left(\sinh\frac{x_3-h}{H}z_m + z_m\cosh\frac{x_3+h}{H}z_m\right.\right. \\
& \left.\left. - (1+z_m^2)^{\frac{1}{2}}\sinh\frac{x_3+h}{H}z_m\right)\right) - z_m\sinh\frac{x_3 z_m}{H}\sinh\frac{hz_m}{H}\Bigg]\Bigg\}\delta_{k\alpha} \\
& - \frac{\delta_{k3}}{2H^2}\,\mathrm{Im}\sum_{m=1}^{\infty} H_0^{(1)}\left(\frac{\rho z_m}{H}\right)\frac{z_m}{(1+z_m^2)^{\frac{1}{2}}-1}\Bigg\{\sinh\frac{hz_m}{H}\cosh\frac{x_3 z_m}{H} \\
& + \frac{hz_m}{H}\left[z_m\sinh\frac{x_3+h}{H}z_m - (1+z_m^2)^{\frac{1}{2}}\cosh\frac{x_3+h}{H}z_m - \cosh\frac{x_3-h}{H}z_m\right] \\
& + \sinh\frac{hz_m}{H}\left((1+z_m^2)^{\frac{1}{2}}\cosh\frac{x_3 z_m}{H} - z_m\sinh\frac{x_3 z_m}{H}\right)\Bigg\}. \qquad (56)
\end{aligned}$$

6. Comparison with the one plane case

It often happens that the singularities which appear in applications are much closer to one of the planes than to the other. This happens for example in modeling ciliated tubes using slender body theory, since there the cilium generally has a length between $\frac{1}{4}$ and $\frac{1}{10}$ the diameter of the tube. In these cases one is tempted to disregard the influence of the second wall and to treat the problem with the solution of the one plane case. This is consistent with the fact that the solution obtained for the two plane case approaches that of the one plane as the distance between the walls becomes relatively greater than the distance of the singularity from one wall.

However to fully justify this procedure an estimate of the closeness of the approximation must be given. To be able to do this, two questions should be answered; how much does the second plane disturb the fields of the one plane case, and for what relations of h/H can we consider the solution of the one plane case a "good" approximation to that of the two planes.

In order to see the effect of the other wall on the drag on a body, one would have to compare forces rather than velocities (which for slender bodies are proportional). If one is

interested in the flow fields produced, when fluid transportation is in mind, velocity fields should be compared. For this purpose, in this section, velocity fields have been plotted for different values of H, including $H = \infty$ (one plane) keeping h constant. It can easily be shown, using the integral representation of the solution, that if we keep ρ and x_3 fixed and let $H \to \infty$, we retrieve the solution for a stokeslet above a flat plate given by Blake [1]. On the other hand, if $(\rho/H) \to \infty$, keeping x_3 and H fixed the solution is entirely different than the one plane case. All u_j^k with either j or k (or both) equal to three (normal to plane) die out exponentially with ρ/H. For a stokeslet parallel to the two planes, the far field is a two-dimensional source doublet of variable strength (as described in the previous section), whereas the far field in the one plane case is a stokes doublet, see Blake and Chwang [4].

In Figure 4, we see the variation of the velocity field u_α^α with the x_3 coordinate for two different values of the pair r_1, r_2; in 4(a) $r_1 = r_2 = h$, in 4(b) $r_1 = 3h$ and $r_2 = 4h$. Measuring at the maximum value of the graphs, we obtain that the disagreement with $H = \infty$ in the first case 4(a), for $H = 4h$, $H = 6h$ and $H = 8h$ is 23%, 14% and 5% respectively. In contrast, the disagreement in the second case 4(b) for $H = 8h$ and $H = 16h$ is 43% and 10% respectively. It is not surprising that in the second case, farther from the singularity, the effect of the wall is stronger, since in the interaction between the singularity

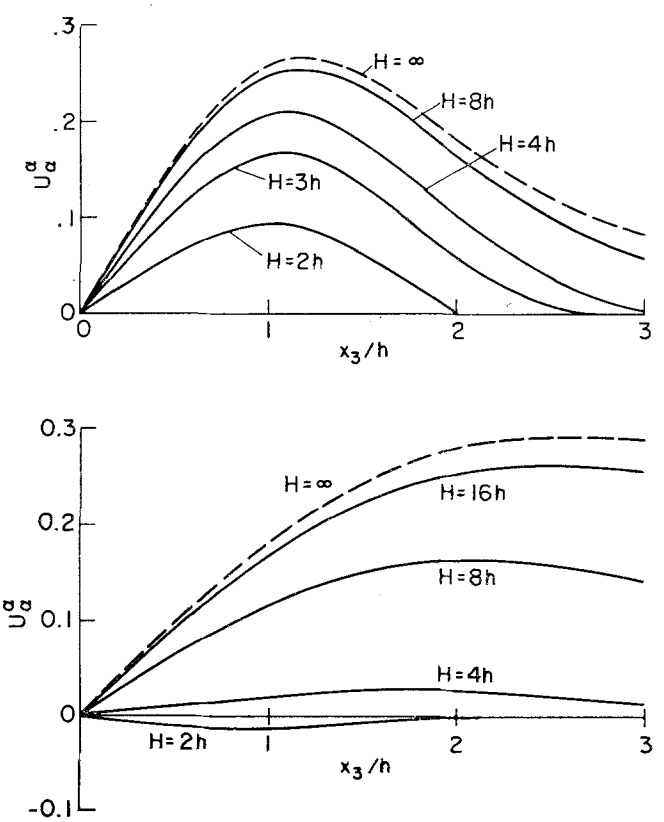

Figure 4. Velocity profiles of u_α^α as a function of the dimensionless coordinate x_3/h, for various values of H (dashed lines represent the one plane case). In (a) the profiles are taken at $r_1 = r_2 = h$ and in (b) at $r_1 = 3h$ and $r_2 = 4h$.

and the wall, each of these factors has a dominant effect near to itself. This can be more clearly seen from Figure 5 which is a plot of the velocity u_α^α against the distance from the singularity for a fixed value $x_3 = 0.5h$. The drastic effect of the wall is also shown here since the graphs with finite H decrease very rapidly.

To illustrate some other components of the velocity field, in Figure 6 we have plotted the velocities u_3^3 in (a), u_3^α in (b) and u_α^3 in (c) against the x_3 coordinate for the pair $r_1 = r_2 = h$.

It is difficult to draw general conclusions from the results obtained in this section since the answers to our original questions will depend on the requirements of each application. However it can be seen that even for the small region $0 < r_1 < h$, $0 < r_2 < h$, $0 < x_3 < 2h$, it is necessary to have at least $H > 8h$ to disregard the effect of the second wall.

7. Conclusion

We have given the Stokes flow field due to a force singularity at an arbitrary location and arbitrary orientation between two parallel plates. Two different forms for the solution were given. One in integral form and the other as a sum of an infinite series. The infinite series form is particularly suited for computations since all series behave like a decreasing exponential and therefore only a few terms are needed even if $\rho/H < 1$. From equation (51) we see that only components parallel to the plates, when the stokeslet is also parallel, do not die out exponentially but have $O[(x_1^2 + x_2^2)^{-1}]$ behaviour. In comparing with the one plane case, it is found that for $H < 8h$, the second wall disturbs the fields of the one plane case considerably in the whole region so to disregard its effect a relation $h/H < \frac{1}{8}$ will be necessary in most cases.

REFERENCES

[1] J. R. Blake, A note on the image system for a stokeslet in a no-slip boundary, *Proc. Camb. Phil. Soc.*, 70 (1971) 303–310.

[2] (a) J. R. Blake, A spherical envelope approach to ciliary propulsion, *J. Fluid Mech.*, 46 (1971) 199–208.
(b) J. R. Blake, Infinite models for ciliary propulsion, *J. Fluid Mech.*, 49 (1971) 209–222.
(c) J. R. Blake, Self-propulsion due to oscillations on the surface of a cylinder at low Reynolds number, *Bull. Aust. Math. Soc.*, 5 (1971) 255–264.

[3] J. R. Blake, A model for the micro-structure in ciliated organisms, *J. Fluid Mech.*, 55 (1972) 1–23.

[4] J. R. Blake and A. T. Chwang, Fundamental singularities of viscous flow, part I, *J. Engineering Math.*, 8 (1974) 23–29.

[5] T. J. Lardner and W. J. Shack, Cilia transport, *Bull. Math. Biophys.*, 34 (1972) 325–335.

[6] H. A. Lorentz, *Zittingsverlag. Akad. v. Wet.*, 5 (1896) 168–182.

[7] N. J. De Mestre, Low-Reynolds-number fall of slender cylinders near boundaries, *J. Fluid Mech.*, 58 (1973) 641–656.

[8] S. M. Ross and S. Corrsin, Results of an analytical model of mucociliary pumping, *J. of Applied Physiology*, 37 (1974) 333–340.

[9] I. N. Sneddon, *Fourier transforms*, McGraw-Hill Co., (1951) 62.

[10] G. N. Watson, *A treatise on the theory of Bessel Functions*, Cambridge Univ. Press, 1948, 2*d* ed.

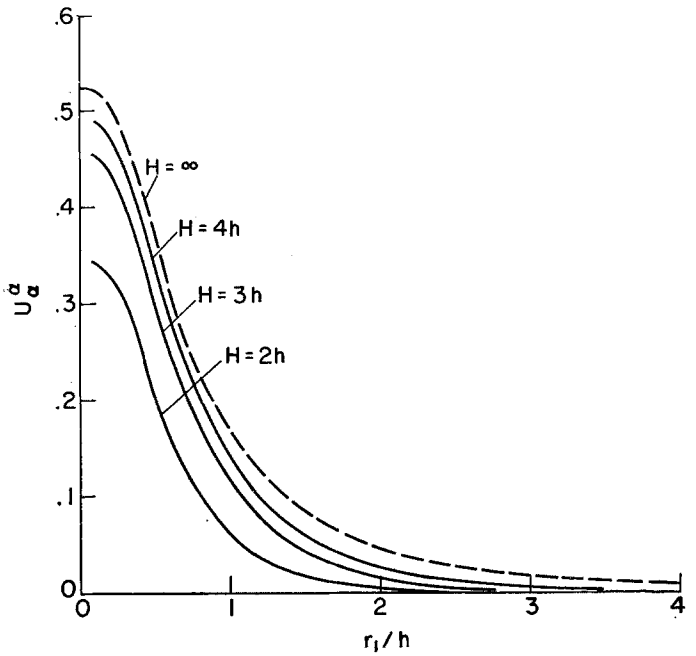

Figure 5. Variation of the velocity u_α^α along the line parallel to the plates $r_1 = r_2$ at a height $x_3 = 0.5h$. As in Figures 4, the dashed line represents the one plane case.

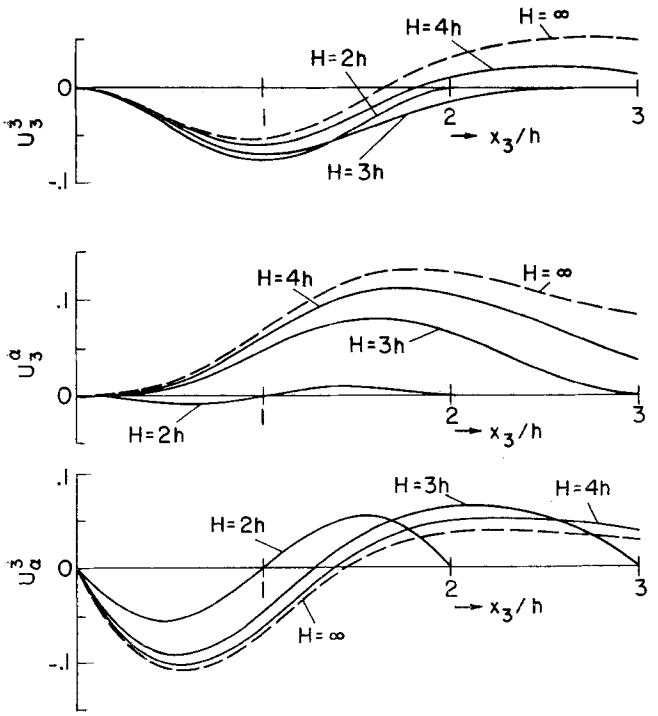

Figure 6. Graphs for three other components of the velocity fields. In (a) u_3^3 is plotted, in (b) u_3^α and in (c) u_α^3. As in 4(a) $r_1 = r_2 = h$.